

# ON THE ADVANTAGES OF PHOTOMETRIC OBSERVATIONS OF THE GEOSTATIONARY SATELLITES AT SMALL PHASE ANGLES

P. P. Sukhov<sup>1</sup>, G. F. Karpenko<sup>1</sup>, K. P. Sukhov<sup>1</sup>, V. P. Epishev<sup>2</sup>, I. I. Motrunych<sup>2</sup>,  
I. Kudzej<sup>3</sup>, P. A. Dubovsky<sup>3</sup>

<sup>1</sup> Astronomical Observatory, Odessa National University, Odessa, Ukraine,  
*psukhov@ukr.net*

<sup>2</sup> Laboratory of Space Research at Uzhgorod National University, Ukraine,  
*lkd.uzhgorod@gmail.com*

<sup>3</sup> Vihorlat Observatory, Humenne, Slovakia, *vihorlatobs1@stonline.sk*

**ABSTRACT.** As a rule, to determine photometric and dynamic characteristics of geostationary satellites required for their identification, long-lasting (from a half of the year to one year) photometric observations are needed at GSS different positions relative to the observer. The authors suggest conducting photometric measurements of GSS when they enter and exit the Earth's shadow near equinoxes. On these dates the GSS brightness increases by several magnitudes, so the use of telescopes with a mirror diameter of 50-70 cm can be effective. For shorter periods it is possible to get more information about the reflective properties of the object than during long-term observations at large phase angles. Several examples of photometric and dynamic characteristics of several GSS obtained near equinoxes are presented here.

**Key words:** multicolour photometry, geostationary satellite, satellite identification, phase angle, equinox, the Earth's shadow.

## 1. Introduction

The Geostationary Earth Orbit (GEO) is overcrowded with space objects (SO) and space debris. There are more than 20 groups of geostationary satellites (GSS) in the GEO that form a compact cluster of several satellites with inclination to the equator and eccentricity close to zero. When re-deploying and manoeuvring geostationary satellites, it is necessary to determine their nationalities, functionalities and types. The highly elliptical orbit (HEO) is poorly monitored. There is no information available for hundreds of objects in that orbit, or they are not reliably determined in catalogues.

In such cases, the SO identification by their orbital parameters is ineffective. This paper describes the advantages of photometric observations of the indicated SO at small phase angles. The SO brightness increases manifold when it enters and exits the Earth's shadow near equinoxes. At a certain time many GSS can be seen with the naked eye.

## 2. Theory

Simultaneous analysis of coordinate and photometric data allows to determine the object's type and its hardware platform, payload, dominant shape and behaviour in orbit (in normal mode and non-standard operation mode) within certain accuracy. It is possible to determine characteristics of the object's failure when it is out-of-order as it was done, for instance, for GSS "Yamal-1" [1], sample return mission "Phobos-Grunt" [2], "DSP F23" [3], "Cosmos 2397" [4], etc.

As a result of the change in geometrical configuration of the "Sun-Earth-GEO" system, the geostationary orbit usually passes outside the Earth's shadow cone throughout a year, except the interims near the vernal and autumnal equinoxes. The longest eclipses of GSS by the Earth's shadow occur on the days when the Sun is close to the vernal and autumnal equinoctial points. The polar regions of the Earth's shadow cross the GSS orbit before and after equinoxes, so duration of its stay in the Earth's shadow gradually shortens down to several minutes. The sunlight reflected off the GSS surface falls on the Earth's surface as a light spot of 350 km in diameter and slowly moves southward in spring and northward in autumn. For the GSS entry into the Earth's shadow two conditions must be met:

$$|\delta_s - \delta_t| < \rho_s, \quad \text{and} \quad |\alpha_s - \alpha_t| < r_t,$$

where  $\delta_s, \delta_t$  – inclination of the GSS orbit and the Earth's shadow axis, respectively;  $\rho_s$  – the diameter of the Earth's shadow cone;  $\alpha_s, \alpha_t$  – the right ascension of SO and the Earth's shadow axis, respectively;  $r_t$  – the length of the chord traversed by a satellite in the shadow.

$$\delta_t = -\delta_o, \quad \alpha_t = \alpha_o - 12^h$$

The most favourable period to record peak-amplitude flares depends on the observer's geographical position. This period lasts about 1.5 days. At around 45° N latitude the dates of GSS flares with maximum amplitudes near the equinoxes fall on the 3<sup>rd</sup> of March and the 12<sup>th</sup> of October [5].

Active GSS with orbital inclination and eccentricity close to zero get regularly eclipsed by the Earth's shadow during 22 days around the equinoxes. The duration of such GSS eclipses by the Earth's shadow depends on the observation date in relation to the equinox and varies from 10 minutes to 72 minutes. And the phase angles can vary from  $13^{\circ}.6$  to  $16^{\circ}.1$  at that [5].

The main photometric, optical, geometrical and dynamic characteristics of GSS, which are used to identify and interpret the SO behaviour in orbit, are as follows:

**Photometric characteristics:** the effective reflective area  $-S\gamma_{\lambda}$ ; spectral reflectance  $\gamma_{\lambda}$ ; phase coefficient  $\beta$  – change in magnitude if  $\psi$  fluctuates by  $1^{\circ}$ ; colour index (B-V, V-R, etc.); magnitude calculated at the phase angle  $\psi = 0^{\circ}$  and reduced to a distance of 36,000 km.

**Optical & geometrical characteristics:** the SO linear dimensions and dominant shape.

**Dynamic characteristics:** the period of rotation around the centre of mass or one of axes; the SO orientation in space determined by the normal vector to the SO glinting surface ( $X_n, Y_n, Z_n$  – the vector's components).

Because of the applied character the satellite's characteristics, not all of them are available to the public. Each of these characteristics does not always unambiguously reply to the question which type an unknown SO belongs to. But the analysis of those characteristics along with orbital data, as well as additional and a priori information allows finding an acceptable solution to identify GSS.

To determine the GSS reflectance characteristics, continuous photometric observations are usually carried out during the whole night. The following problems can arise in the course of those observations:

1. Geostationary satellites are very faint with brightness of about  $12^m$ - $15^m$  at the phase angles  $\psi > 30^{\circ}$ . To photometrically such GSS, it is necessary to use telescopes with primary mirror diameter of approximately 1 m and larger.

2. When conducting simultaneous basic observations with reference distance of hundreds or thousands of kilometres at  $\psi > 30^{\circ}$ , each observer can see the SO at a different angle. It is not quite correct to compare or combine the light curves obtained at different observation sites to interpret the SO behaviour over time in the orbit at a certain moment of observation. Simultaneous basic observations also often restricted by weather conditions at the observation sites.

The experience gained by the authors of this paper shows that the photometry of GSS at small phase angles near equinoxes considerably saves time required to obtain the GSS characteristics and allows to improve the content and quality of the target information. The GSS brightness can increase by  $10^m$  during these days, so it can be effective to use telescopes with a mirror diameter of 50-70 cm in diameter. The analysis of light curves at small  $\psi$  for objects with diffuse and specular components also enables to obtain more reliable reflectance characteristics of the satellite's surface.

The observed magnitude  $m$  of a satellite depends mainly on three parameters: the reflective area GSS  $-S$ , reflectance characteristics his surface  $-\gamma_{\lambda}$ , and the phase angle  $-\psi$ .

$$m = F \{ \psi, S, \gamma_{\lambda} \}.$$

It is possible to determine  $m$  from the observation data and calculate the phase angle  $\psi$ . The computation of the spectral reflectance  $-\gamma_{\lambda}$  and apparent effective reflective area  $-S$  is quite probabilistic and depends on many reasons listed below.

The GSS brightness in terms of magnitude is calculated by famous Pogson's formula:  $m_{\lambda} = -2.5 \lg E_1/E_2$ . As per McCue et al. [6], the GSS brightness in the target wavelength range can be expressed as the following formula:

$$m_{\lambda} = m_{\lambda}^c - 2,5 \lg \left[ \frac{S\gamma_{\lambda}F(\psi)}{d^2} \right]. \quad (1)$$

where  $m_{\lambda}^c$  – the Sun's magnitude in the wavelength range,  $S$  – the area of the GSS surface illuminated by the Sun and thus visible to an observer,  $\gamma_{\lambda}$  – spectral reflectance,  $S\gamma_{\lambda}$  – effective reflective area,  $\psi$  – satellite-centric phase angle,  $F(\psi)$  – phase function,  $d$  – topocentric distance to the object. The Moon's illumination, light reflection and scattering by the Earth are left out of formula (1). At an altitude of 36,000 km the interference of the Earth's background illumination, including absorption and Rayleigh scattering, is negligible and makes up hundredths of magnitude [7, 8]. The Moon's background illumination can be neglected as the GSS photometry is feasible at large angular distances to the Moon and at small lunar phases.

The shape of the GSS light curve on its entering (exiting) the Earth's shadow is primarily related to the effective reflective area  $S\gamma_{\lambda}$ . Its value depends on the optical characteristics of the SO surface, under-satellite point longitude, satellite's orientation, geographical position of an observer, season and the satellite's orbit life (ageing of the materials used in the satellite's construction), etc.

At small phase angles ( $\cos \psi \approx 1$ ) when the reflective area is maximum, values  $S\gamma_{\lambda}$  and  $\gamma_{\lambda}$  for objects of known dimensions can be calculated using the observation data. As follows from formula (1):

$$S\gamma_{\lambda} = d^2 \cdot 10^{\frac{m_{\lambda}^c - m_{\lambda}}{2.512}} \cdot \sec \psi.$$

The value  $\gamma_{\lambda}$  is determined in a similar manner:

$$\gamma_{\lambda} = \frac{d^2}{S} 10^{\frac{m_{\lambda}^c - m_{\lambda}}{2.5}}.$$

Thus, with known GSS dimensions, it is possible to determine its near-real effective reflective area  $-S\gamma_{\lambda}$  and spectral reflectance  $\gamma_{\lambda}$ . With known dominant geometric configuration, it is possible to use corresponding scattering phase functions, particularly for sphere, cylinder, plate, etc.

The phase function of a satellite, except spherical one, assumes that its space orientation is known. The satellite's orientation in space is determined by the normal vector to the visible part of the SO surface that generates a flare at the time of observation in the satellite-centric coordinate system. The normal vector components are  $X_n, Y_n$  and  $Z_n$ . The X-axis is parallel to the celestial equator and oriented to the vernal equinox point. The Y-axis is oriented to the Earth's centre. The Z-axis is oriented to the celestial pole parallelly to the Earth's rotational axis. The satellite identification by the photometric observations can be conducted in two ways.

**Direct problem.** The apparent brightness of an object at any specific time is computed and further analysed by the GSS estimated (known) shape, lighting conditions and optical properties of its surface, as well as by known SO orientation relative to an observer. This problem is practically solvable with rather high probability.

**Reverse problem.** In this case the non-uniqueness in determination of the SO shape by its light curve is associated with the following fundamental principle. The algorithm input is a function dependent on a single argument as phase angel - brightness (or  $m(t)$ ). In mathematics such a problem is classified as incorrect, and the obtained solutions are generally unstable or have no physical meaning.

However, the problem can be simplified if the object's dominant shape is known. The phase curve of the defined shape of the object is described by the scattering function  $F(\psi)$  for basic geometrical figures (plate, cylinder, sphere, etc.). They are analytically determined in the studies by E.R.Lanczi, W.R.Rambauske, G.A.McCue, J.G.Williams, J.M.Morford [6, 9, 10]. The GSS orientation in space can be determined by mirror flares using the method described by V.Epishhev in [11].

### 3. Results

The computation of some photometric and dynamic characteristics of several GSS at small  $\psi$  was preformed.

About 50 multicolour light curves in B, V, R filters (Johnson's system) for the GSS "Intelsat 10-02" entering and exiting the Earth's shadow have been obtained in Odessa Astronomical Observatory (Ukraine) and Vihorlat Observatory (Slovakia) during 2005-2014. A photomultiplier FEU-79 operated in the photon-counting mode was used to measure the satellites' brightness. The in-depth study of the mentioned GSS behaviour in orbit on the basis of multicolour observations is reported in [12].

"Intelsat 10-02" is based on the "Eurostar 3000" platform; its solar panel (SP) span is 45 metres. The GSS light curves is best approximated by the phase functions for a flat plate with Lambertian reflectance, which takes the form:

$$F(\psi) = \cos \varepsilon \cdot \cos \theta,$$

where  $\varepsilon$  and  $\theta$  correspond to the angles of incidence and reflection of the light to plane of the SP, respectively.

The "short" light curve (obtained with 50-cm telescope in Odessa, Ukraine) is shown in Figure 1a; and the "long" light curve (obtained with 1-m telescope in Humenne, Slovakia) is presented in Figure 1b.

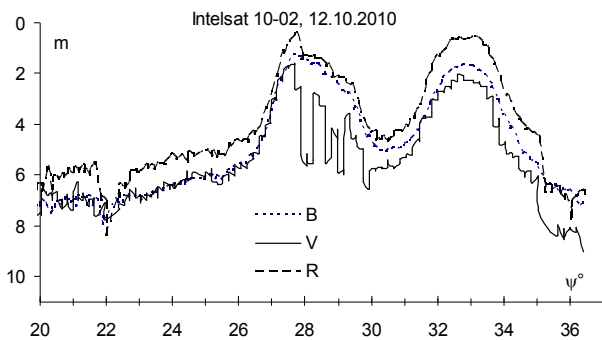


Figure 1a: Odessa – "Short" phase light curve at the time of exit from the Earth's shadow

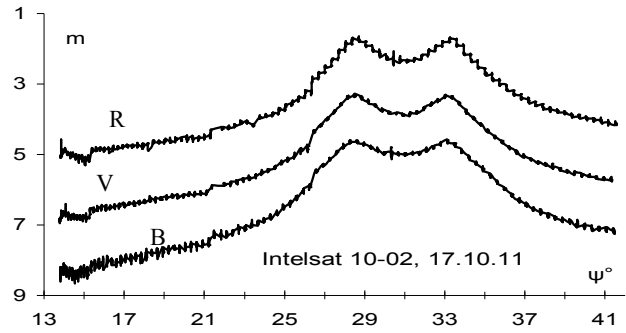


Figure 1b: Slovakia – "Long" phase light curve at the time of exit from the Earth's shadow

In the opinion of the authors of [12], the presence of two brightness peaks on the light curve is attributed to the contribution in the total quasi-mirror reflected light of the first panel SP, and then by that of the second panel SP. The brightness decrease between the two peaks can be explained by the movement of the solar image on the payload platform. The analysis of the data presented in Table 1 reports that the SO functioned normally during the periods of observations.

Table 1: The results of the solar panels' orientation determination at the time of the GSS peak brightness

Observation date	UT	$\alpha_{\odot}, ^\circ$	$\delta_{\odot}, ^\circ$	$\alpha_{\text{obs}}, ^\circ$	$\delta_{\text{obs}}, ^\circ$	$\alpha_{\text{n}}, ^\circ$	$\delta_{\text{n}}, ^\circ$
06.10.2010	1 <sup>h</sup> 43 <sup>m</sup> 54 <sup>s</sup>	191.56	-5.02	216.37	6.82	204.01	0.92
	2 <sup>h</sup> 08 <sup>m</sup> 13 <sup>s</sup>	191.71	-5.03	222.44	6.82	207.05	0.92
07.10.2010	1 <sup>h</sup> 43 <sup>m</sup> 22 <sup>s</sup>	192.48	-5.40	217.21	6.82	204.89	0.72
	2 <sup>h</sup> 06 <sup>m</sup> 00 <sup>s</sup>	192.62	-5.40	222.81	6.82	207.72	0.72
12.10.2010	1 <sup>h</sup> 37 <sup>m</sup> 55 <sup>s</sup>	197.05	-7.30	220.76	6.82	208.97	-0.23
	2 <sup>h</sup> 02 <sup>m</sup> 24 <sup>s</sup>	197.20	-7.31	226.88	6.82	212.03	-0.23
14.10.2010	1 <sup>h</sup> 59 <sup>m</sup> 58 <sup>s</sup>	199.05	-8.05	228.28	6.82	213.68	-0.63

The first two columns of the Table are clear. The following data are presented in the next columns: satellite-centric equatorial coordinates of the Sun ( $\alpha_{\odot}$ ,  $\delta_{\odot}$ ), observer ( $\alpha_{\text{obs}}$ ,  $\delta_{\text{obs}}$ ) and normal orientation towards the solar panel ( $\alpha_{\text{n}}$ ,  $\delta_{\text{n}}$ ). All angles are measured in degrees.

Values  $\gamma_{\lambda}$  and  $(S\gamma_{\lambda})$  reduced to a distance of 36,000 km and  $\psi = 0^\circ$  for "Intelsat 10-02" are given in Table 2; the values were computed by the "short" light curve with the variation range  $\psi \approx 13^\circ$  and by the "long" light curve with the variation range  $\psi \approx 28^\circ$  (marked with symbol \*).

Table 2: The  $(S\gamma_{\lambda})$ , and spectral reflection coefficient  $\gamma_{\lambda}$ , computed by the "short" and "long" light curves

Sp	$\gamma_{\lambda}$ ±0.02	* $\gamma_{\lambda}$ ±0.02	$(S\gamma_{\lambda})$ , m <sup>2</sup> ±1.0	* $(S\gamma_{\lambda})$ , m <sup>2</sup> ±0.60
B	0.18	0.18	17.58	16.25
V	0.34	0.38	32.44	34.11
R	0.22	0.21	20.26	19.15

As is seen, the values  $\gamma_{\lambda}$  and  $(S\gamma_{\lambda})$  computed by the "short" and "long" light curves are similar.

The values  $S\gamma_\lambda$  and  $\gamma_\lambda$  for GSS of two types with “Eurostar 3000S” (“Skynet-5B”, “Skynet-5A”, “Skynet-5D”) and “GeoBus” (“Sicral-1” and “Sicral-1B”) platforms were computed by the “short” light curves in a similar way (see Table 3). There were at least three light curves obtained for each object on its entry and exit from the Earth’s shadow.

Table 3: The effective reflective area  $S\gamma_\lambda$  and spectral reflectance  $\gamma_\lambda$  for GSS with platforms of different types computed by the “short” light curves

Platform types	SP	$\gamma_\lambda$	$S\gamma_\lambda, m^2, \psi = 0^\circ$
Eurostar 3000	B	$0.18 \pm 0.02$	$17.58 \pm 1.00$
	V	$0.34 \pm 0.02$	$32.44 \pm 1.00$
	R	$0.22 \pm 0.02$	$20.26 \pm 1.00$
Eurostar 3000S	B	$0.14 \pm 0.02$	$11.86 \pm 0.50$
	V	$0.11 \pm 0.02$	$9.74 \pm 0.50$
	R	$0.12 \pm 0.02$	$10.80 \pm 0.50$
GeoBus (Italsat-3000)	B	$0.12 \pm 0.05$	$5.41 \pm 1.60$
	V	$0.12 \pm 0.05$	$5.17 \pm 1.60$
	R	$0.14 \pm 0.05$	$6.22 \pm 1.60$

The “short” phase light curves for GSS of two types, “Sky-net-5B” and “Sicral-1B” are shown in Figures 2a and 2b.

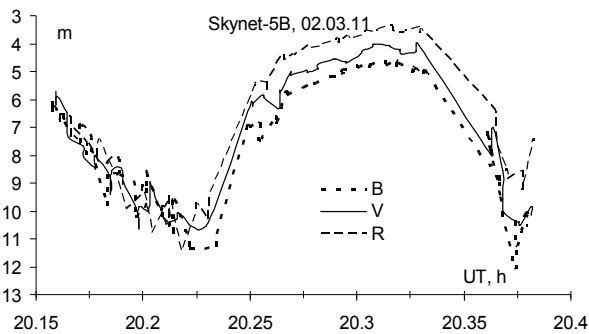


Figure 2a: The “short” phase light curve after satellite’s exit from the shadow

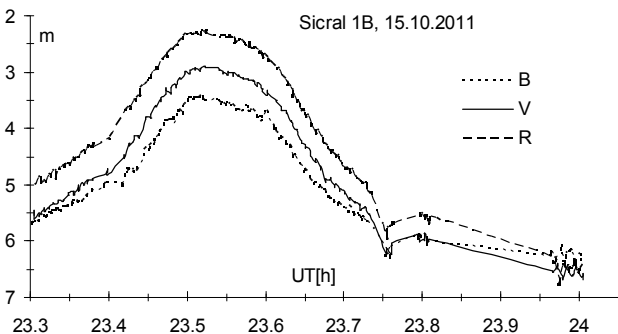


Figure 2b: The “short” phase light curve after satellite’s exit from the shadow

The Table 3 shows; the values  $S\gamma_\lambda$  and  $\gamma_\lambda$  for the “Skynet» (with “Eurostar 3000S platform) and «Sicral» (GeoBus Italsat-3000) military satellites are several times less than those for communication satellites with “Eurostar 3000” platform; that corresponds to reality.

Three light curves at small  $\psi$  were obtained for the emergency GSS “Cosmos 2397”. The most meaningful phase light curve with diffuse and specular components for that SO after its exit from the Earth’s shadow is given in Figure 3. The presence of four peaks in Figure 3b appears to indicate the presence of four segments of SP. The solar panels rotate with maximum speed of one rotation per 18 minutes. At the time of the first flare the solar panels’ tilt towards the Sun was 6.5 degrees, and at the time of the second flare – 8.7°. The minimum inclination of the panels towards the Sun was  $\sim 5.0^\circ$ . That is classical inclination of the active GSS solar panels towards the Sun. The solar panels’ orientation remains unaltered relative to the Sun, although the satellite slowly drifts along the orbit ( $\sim 1^\circ$  per day). The components of unit normal vector to the SP surface in the light curve segment corresponding to the second peak in brightness at  $\psi$  from  $19.13^\circ$  to  $23.65^\circ$  are given in Table 4. As can be seen from Table 4, the Yn component is practically oriented to the observer. The SP orientation by two mirror flares in Figure 3a demonstrates that they were moving practically in the ecliptic plane. Thus, the normal orientation for the first flare was  $a = 176.96^\circ, \delta = 4.94^\circ$ , and for the second flare  $a = 179.22^\circ, \delta = 4.96^\circ$ .

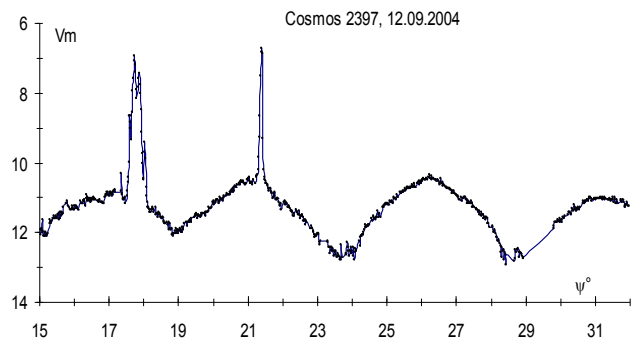


Figure 3a: The phase light curve after satellite’s exit from the shadow

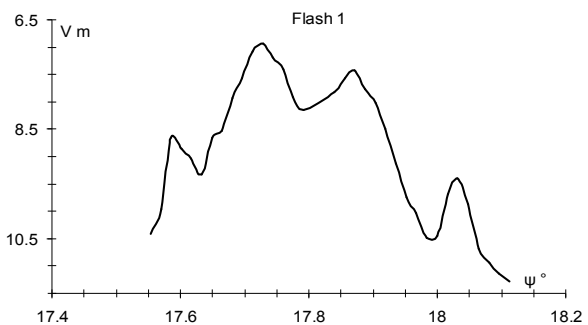


Figure 3b: A segment of the first flare

Table 4: The normal vector orientation towards SP related to the observer at the phase angles from 19°.13 to 23°.65 as of 12.09.2004.

$\Psi^\circ$	$X_n$	$Y_n$	$Z_n$
19.130	0.023	0.994	0.104
20.196	0.013	0.995	0.096
21.044	0.004	0.996	0.090
21.413	0.001	0.996	0.088
21.766	0.003	0.996	0.086
22.855	0.014	0.997	0.081
23.652	0.021	0.997	0.077

With  $\Psi^\circ$  – the satellite-centric phase angle;  $X_n$ ,  $Y_n$ ,  $Z_n$  – components of the normal vector to the reflective surface. The effective reflective area for the solar panels at the given SO angle for the time of the first flare (see Figure 3b) were computed:  $S_{\gamma_1}=0.87 \text{ m}^2$ ,  $S_{\gamma_2}=4.18 \text{ m}^2$ ,  $S_{\gamma_3}=2.67 \text{ m}^2$ ,  $S_{\gamma_4}=0.66 \text{ m}^2$ , where  $S_{\gamma_i}$  – the number of the panel, for which the effective reflective area were determined.

*Possible cause of non-standard operation mode.* The period of the object’s rotation around the Z component is 18 minutes whilst making a cone with an angle close to 5° and causing a change in the measured brightness (mainly reflected off the solar panels) with amplitude of about 2.0<sup>m</sup>. The most likely is that the GSS stabilization is upset, and that resulted in its rotation around the axis with orientation close to that one of the Z-axis [4].

On the basis of the photometric observations, the authors of study [3] identified the breakdown of satellite "DSP F23". "The analysis of the light curves and behaviour of the normal orientation to the specular reflecting elements, first of all to  $Z_n$ , indicates that the satellite practically maintains its orientation to the Earth's centre, but there is no spin around that axis with a period close to 10 seconds. That resulted in inability to scan the Earth's surface that was the main purpose of the SO and caused its change-over to the librational mode".

#### 4. Advantages and Conclusions

In the authors’ opinion, the main advantages of the GSS photometry the near equinoxes are the following:

1. It is possible to get a few tens of light curves enter and out from of the Earth's shadow during the night.
2. It is possible to determine almost all reflectance and

dynamic characteristics, except the phase coefficient  $\beta$ .

3. More reliable photometric and dynamic data for objects of known dimensions can be computed.

4. The GSS behaviour in orbit, either in normal mode or non-standard operation mode, can be estimated by its mirror flares.

5. It is possible to considerably save time to obtain data characteristics of GSS, which are necessary to identify an unknown GSS.

The photometric database (Johnson’s system) of the Astronomical Observatory of I.I.Mechnikov Odessa National University includes about 500 light curves for more than 100 GSS of different types: “Intelsat”, “DSP”, “SBIRS”, “Eutelsat”, “Mentor”, “Express”, “Skynet”, “Yamal”, “Sicral”, “Mercury”, “PAN”, etc.

#### References

Bagrov A.V., Vygon V.G., Rykhlova L.V., Shargorodskiy V.D.: 2000, in: *The Near-Earth Astronomy and Issues in the Study of Small Solar System Bodies* (in Russian). M.: Kosmosinform, 276 p.

Yepishev V.P., Barna I.V., Bilinskiy A.I., Koshkin N.I., Kudak V.I., Lopachenko V.N., Martynyuk-Lototskiy K.P., Motrunich I.I., Naybauer I.F., Rykhal'skiy V.V.: 2013, in *International Scientific Conference the Near-Earth Astronomy* (in Russian), Krasnodar, Kuban State Univ. Press, 129.

Didenko A.V., Usol'tseva L.A.: 2010, in *Proc. of the National Academy of Sciences of the Republic of Kazakhstan. The Physical and Mathematical Series* (in Russian), **No. 4**, 81.

Sukhov P.P., Movchan A.I., Kochkin N.I., Korniychuk L.V., Strakhova S.L., Epishev V.P.: 2004, *Odessa Astron. Publ.*, **17**, 99.

Karpenko G.F., Murnikov B.A., Sukhov P.P.: 2009/2010, *Odessa Astron. Publ.*, **22**, 25.

McCue G.A., Williams J.G., Morford J.M.: 1971, *Planet. and Space. Sci.*, **19**, 851.

Severnyy S.A., Smirnov M.A., Bagrov A.V.: 1986, *Scientific Inform. of the Astr. Council of the Academy of Sciences of USSR*, (in Russian), **58**, 103.

Smirnov M.A.: 1994, *Photometric Observations of Artificial Celestial Bodies*. Thesis of the Doctor of Phys. and Mathemat. Sci., Institute of Astronomy of the Academy of Sciences of Russian Federation (in Russian), 164 pp.

Lanczi E.R.: 1966, *J. Opt. Soc. Am.*, **56**, 873.

Rambauske W.R., Gruenzel R.R.: 1965, *J. Opt. Soc. Am.*, 1965, **55**, 315.

Yepishev V.P.: 1983, *Astrometry and Astrophysics*, Academy of Sci. of USSR (in Russian), 89.

Sukhov P.P., Karpenko G.F., Epishev V.P., Motrunych I.I.: 2009/2010, *Odessa Astron. Publ.*, **22**, 55.